

The **next generation** GBCA  
from Guerbet is here

Explore new possibilities >

Guerbet | 

© Guerbet 2024 GUOB220151-A

# AJNR

## **Use of CT Angiography for Anatomic Localization of Arteriovenous Malformation Nidal Components**

V. Gupta, M. Chugh, B.S. Walia, S. Vaishya and A.N. Jha

*AJNR Am J Neuroradiol* 2008, 29 (10) 1837-1840

doi: <https://doi.org/10.3174/ajnr.A1136>

<http://www.ajnr.org/content/29/10/1837>

This information is current as  
of August 9, 2024.

V. Gupta  
M. Chugh  
B.S. Walia  
S. Vaishya  
A.N. Jha

# Use of CT Angiography for Anatomic Localization of Arteriovenous Malformation Nidal Components

**SUMMARY:** We report a case of diffuse arteriovenous malformation (AVM) in basal ganglia and an internal capsule associated with venous aneurysms. The patient was treated by embolization guided by CT angiography to target the basal ganglionic portion of the AVM while sparing the internal capsule. Our case demonstrates that it is possible to obtain good quality intranidal angiograms by using CT angiography, which can be useful for exact localization of the catheterized part of the nidus.

A new combined angiography/CT suite has been developed that uses flat-panel detector technology for higher-resolution angiography that is also capable of producing cone-beam volume CT.<sup>1-4</sup> We report a case of diffuse arteriovenous malformation (AVM) in basal ganglia and an internal capsule treated by targeted embolization guided by CT angiography (CTA). The CTA was useful for anatomic localization of the nidal components, which would have been difficult to determine only by the angiographic criteria. The technique enabled us to perform precise targeted embolization of the desired nidal components so as to decrease the risk of serious neurologic injury in our case of diffuse AVM involving vital structures.

## Technique

A 30-year-old male patient presented with sudden severe headache along with vomiting. Head CT revealed intraventricular hemorrhage. The patient had a known case of left basal ganglia AVM. He had initially presented with intraventricular hemorrhage 9 years ago and had been treated with stereotactic radiosurgery at another institution. However, no follow-up angiograms had been done. Repeat digital subtraction angiography (DSA) revealed an AVM involving the left basal ganglia, internal capsule, and periventricular white matter with feeders from left lateral and medial lenticulostriate arteries arising from the middle and anterior cerebral arteries. A small feeder was also seen from the thalamostriate branch of the posterior cerebral artery. The malformation was draining through ventricular veins into the internal cerebral vein. An aneurysm was seen in the draining vein along with an outpouching from its superior aspect suggestive of a pseudoaneurysm. The patient was referred to our institution for embolization of the AVM. Angiographic features of ill-defined and patchy nidus suggested a diffuse malformation. MR imaging showed scattered flow voids (Fig 1A) with normal parenchyma interspersed in between the flow voids, suggesting a diffuse AVM. We planned partial targeted embolization to reduce the risk of hemorrhage from the venous aneurysm.

A guiding catheter (Guider 6F; Boston Scientific, Fremont, Calif) was placed in the left internal carotid artery (ICA). DSA revealed the AVM as described above (Fig 1B–D); however, in comparison with

the previous angiogram, the pseudoaneurysm had increased in size (arrow, Fig 1C). Under roadmap guidance, a microcatheter (Magic 1.2FM; Balt Extrusion, Montmorency, France) was navigated into the AVM nidus through the lenticulostriate feeder by using a microguidewire (Mirage 0.008; ev3, Irvine, Calif). Microcatheter injections revealed a diffuse vascular blush with some irregular vessels and arteriovenous shunting (Fig 2A). In view of the diffuse nidus, parenchymal injury was expected during embolization. To decrease the chances of neurologic deficit, we decided to target the basal ganglionic portion of the AVM while sparing the internal capsule. For exact anatomic localization of the part of AVM to be embolized, CTA was performed during the microcatheter injection.

CTA was performed by using a flat panel detector angiographic system (Axiom Artis dBA; Siemens Medical Solutions, Forchheim, Germany) with commercially available software (DynaCT; Siemens Medical Solutions). During the acquisition, 0.5 mL of contrast diluted by 75% with normal saline was injected through the microcatheter. Image postprocessing was performed to correct scattered radiation, beam hardening, and ring artifacts on a commercially available workstation (Leonardo; Siemens Medical Solutions). These images were available for evaluation in 3–4 minutes and could be evaluated in all 3 of the planes.

Intranidal CTA revealed opacification of basal ganglia sparing the internal capsule (Fig 2B, -C). Thereafter, the feeder was embolized (Fig 2D) with *n*-butyl 2-cyanoacrylate (B. Braun, Tuttlingen, Germany) diluted by 80% with lipiodol (Gurbert, Aulnay-sous-Bois, France). The patient did not have any fresh neurologic deficits after the embolization. Postembolization MR imaging revealed altered signal intensity in the left basal ganglia (Fig 2E) with restricted diffusion on apparent diffusion coefficient mapping (data not shown), suggesting an acute ischemic change in the embolized area.

Repeat angiogram after 2 months revealed a marked reduction in the size of the venous aneurysm with complete thrombosis of the suspected pseudoaneurysm (Fig 2F). Further embolization was performed via the lenticulostriate feeders (Fig 3A). CTA with contrast injection in the feeder from the posterior cerebral artery revealed opacification of the internal capsule and, therefore, was not embolized (Fig 3B).

## Discussion

CTA technology is likely to be useful in intracranial endovascular procedures, such as aneurysm embolization, intra-arterial thrombolysis, and intracranial AVM embolization, to exclude intracranial hemorrhage or change in ventricular size and mass effect.<sup>2</sup> This technology is also being used for clear visualization of stents in both intracranial and extracranial arteries.<sup>3,4</sup> In our case, CTA during microcatheter injection

Received January 3, 2008; accepted after revision February 1.

From the Departments of Interventional Neuroradiology (V.G., M.C.) and Neurosurgery (B.S.W., S.V., A.N.J.), Max Institute of Neurosciences, Max Superspeciality Hospital, New Delhi, India.

Please address correspondence to Vipul Gupta, Interventional Neuroradiology, Max Institute of Neurosciences, Max Superspeciality Hospital, 1 Press Enclave Rd, Saket, New Delhi, India 110017; e-mail: vipulgupta25@yahoo.com

DOI 10.3174/ajnr.A1136

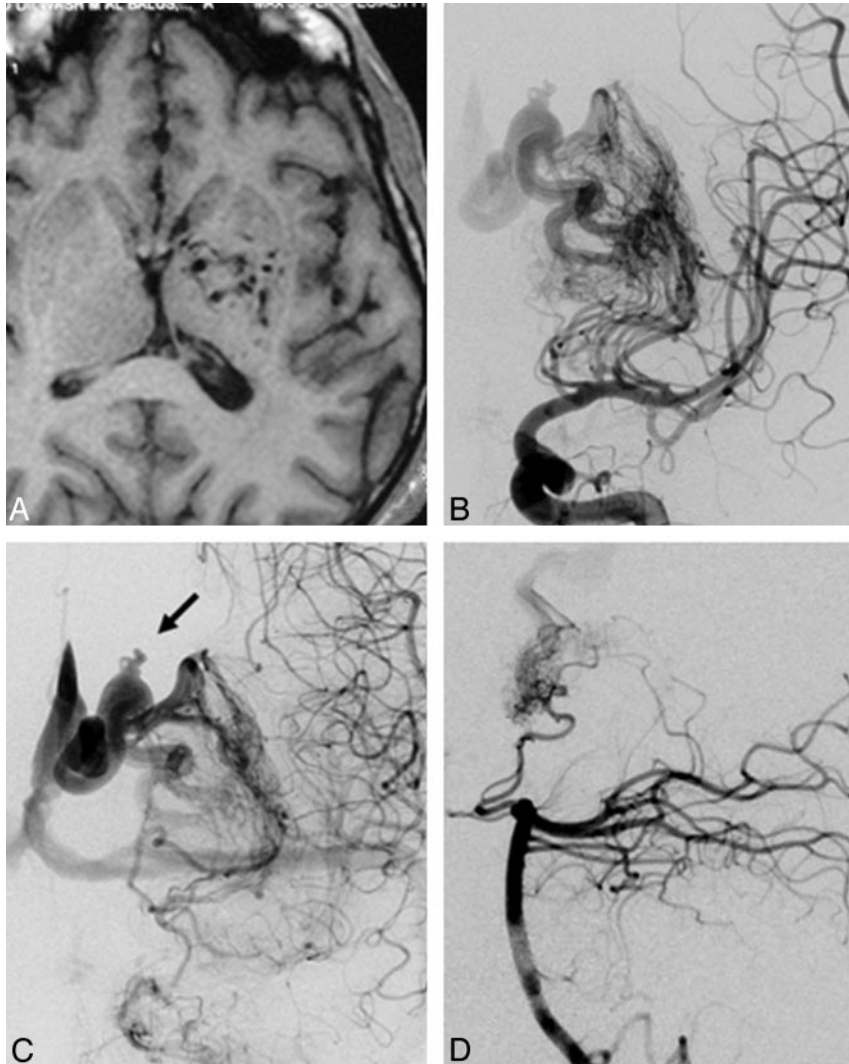


**Fig 1.** MR image (T1-weighted, axial) shows scattered flow voids in left basal ganglia and internal capsule without a well-defined nidus, suggestive of a diffuse AVM (A). DSA image (left ICA injection, anteroposterior view) shows an ill-defined AVM in left basal ganglia and internal capsule (B). Venous phase shows aneurysmal dilation in draining vein along with an out-pouching (arrow, C). Left vertebral artery injection (lateral view) shows part of the AVM fed by hypertrophied thalamostriate perforator arising from posterior cerebral artery (D).

helped us in performing precise targeted embolization of the AVM nidus.

Diffuse AVMs are regarded as a specific subset within the gamut of cerebral AVMs. Unlike the typical AVMs, these lesions contain normal cerebral tissue between the abnormal vessels.<sup>5</sup> Characteristic angiographic features included multiple small arterial feeders, small ectatic vessels in the malformation itself, multiple small draining veins, and a diffuse, puddling appearance of the contrast dye.<sup>5</sup> Because of the intervening parenchyma and ill-defined nidus, treatment by any means can result in injury to normal tissue.<sup>6</sup> In our case, the vascular malformation involved the deep nuclei and internal capsule, with a high possibility of neurologic deficit in the event of parenchymal injury. However, history of repeated intracranial bleeding and the presence of a large venous aneurysm, along with a pseudoaneurysm, made it imperative to treat the malformation. The size, location, and diffuseness of the nidus excluded surgery. Radiosurgery had failed previ-

ously in our case, and the relative lack of effectiveness of radiosurgery in the treatment of diffuse AVMs has been reported in the literature.<sup>7</sup> Repeat radiosurgery in therapeutic doses carried a high risk of neural injury, and we planned to do targeted partial embolization.

During embolization, the basal ganglionic portion of the AVM was targeted while avoiding the pyramidal tracts in the internal capsule. CTA was extremely useful in performing precise embolization of the desired part of the malformation. Follow-up angiogram after partial targeted embolization showed reduction of size of the venous aneurysm along with thrombosis of the pseudoaneurysm.

Our case demonstrates that it is possible to obtain good quality intranidal angiograms by using CTA while using a minimal contrast dose. This technique is not only useful for anatomic localization of the catheterized part of nidus but is also likely to be useful to study the angioarchitecture of the AVM nidus, feeding arteries, and draining veins.

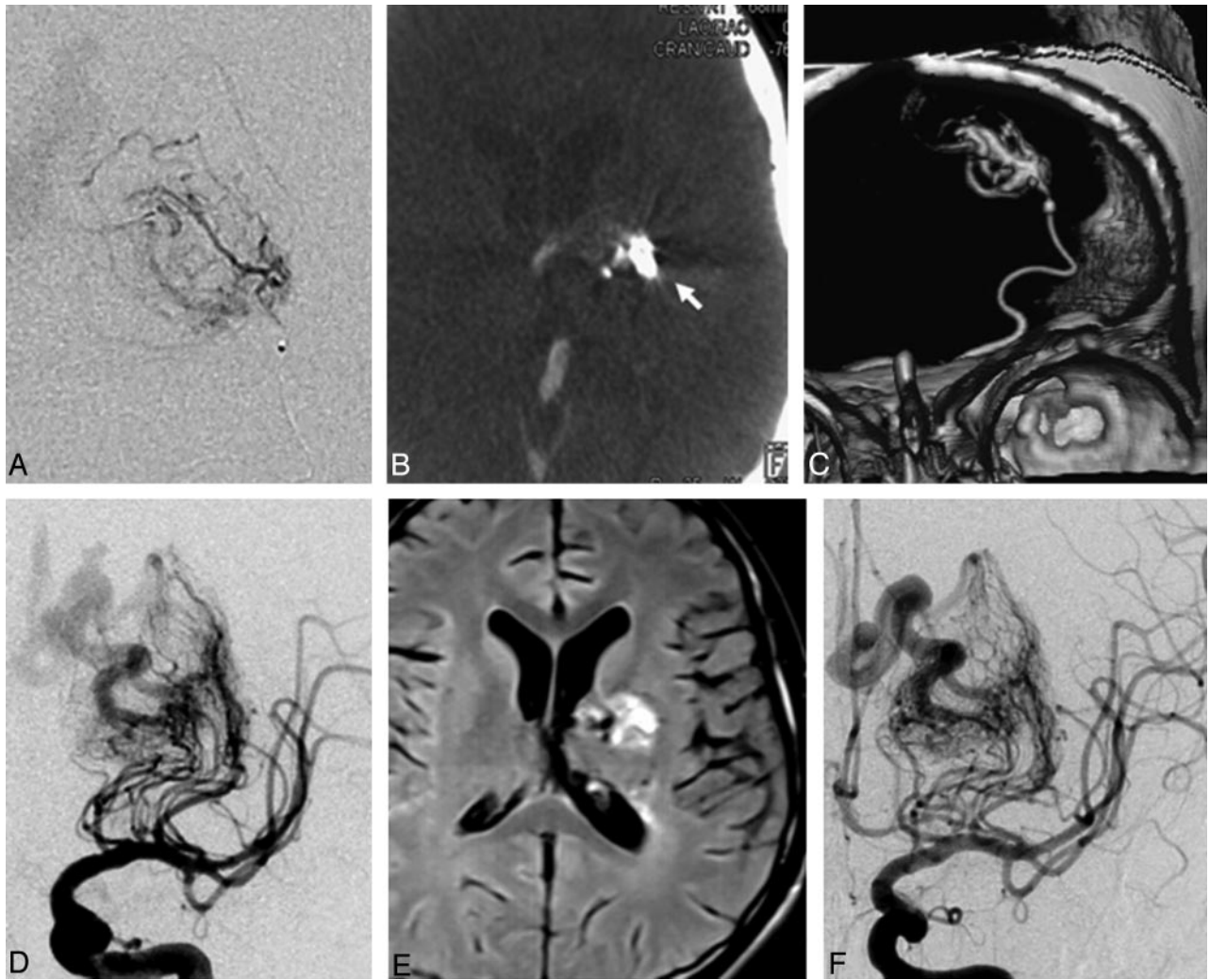


**Fig 2.** Microcatheter injection in the lenticulostriate artery shows patchy vascular network consistent with diffuse nature of AVM nidus (A). CTA was performed during contrast injection from microcatheter. Axial CTA image shows the nidus opacification in left basal ganglia sparing the internal capsule (arrow, B). Reconstruction with volume rendering technique (VRT) clearly shows the microcatheter and vascular network (C). Postembolization ICA angiogram shows obliteration of middle third of nidus (D). Postembolization MR (fluid-attenuated inversion recovery, axial image) showed fresh signal intensity change in the embolized portion of the basal ganglia (E). Left ICA angiogram performed 3 months after embolization shows marked shrinkage of the venous aneurysm with complete thrombosis of the pseudoaneurysm (F).

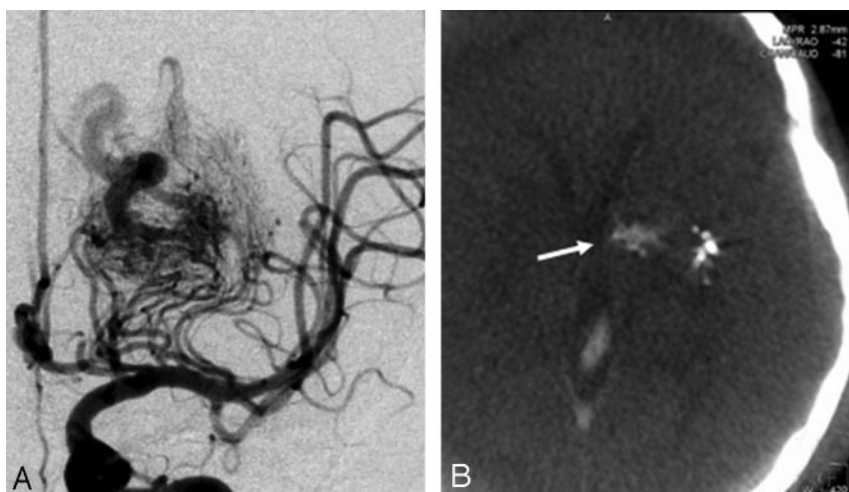


**Fig 3.** Left ICA angiogram after second session of embolization shows marked reduction in the size of nidus with slow opacification of the draining veins (A). CTA performed with microcatheter injection in the thalamostriate feeder showed opacification of internal capsule (arrow) medial to the glue cast (B).

## References

1. Akpek S, Brunner T, Benndorf G, et al. **Three-dimensional imaging and cone beam volume CT in C-arm angiography with flat panel detector.** *Diagn Interv Radiol* 2005;11:10–13
2. Heran NS, Song JK, Namba K, et al. **The utility of DynaCT in neuroendovascular procedures.** *AJNR Am J Neuroradiol* 2006;27:330–32
3. Benndorf G, Strother CM, Claus B, et al. **Angiographic CT in cerebrovascular stenting.** *AJNR Am J Neuroradiol* 2005;26:1813–18
4. Richter G, Engelhorn T, Struffert T, et al. **Flat panel detector angiographic CT for stent-assisted coil embolization of broad-based cerebral aneurysms.** *AJNR Am J Neuroradiol* 2007;28:1902–08
5. Chin LS, Raffel C, Gonzalez-Gomez I, et al. **Diffuse arteriovenous malformations: a clinical, radiological, and pathological description.** *Neurosurgery* 1992;31:863–68
6. Du R, Keyoung HM, Dowd CF, et al. **The effects of diffuseness and deep perforating artery supply on outcomes after microsurgical resection of brain arteriovenous malformations.** *Neurosurgery* 2007;60:638–46
7. Zipfel GJ, Bradshaw P, Bova FJ, et al. **Do the morphological characteristics of arteriovenous malformations affect the results of radiosurgery?** *J Neurosurg* 2004;101:393–401